Slow dynamics in a primitive tetrahedral network model

Cristiano De Michele[a)]
Dipartimento di Fisica and INFM-CNR-SOFT, Università di Roma La Sapienza, Piazzale A. Moro 2, 00185 Roma, Italy

Piero Tartaglia
Dipartimento di Fisica and INFM-CNR-SMC, Università di Roma La Sapienza, Piazzale A. Moro 2, 00185 Roma, Italy

Francesco Sciortino
Dipartimento di Fisica and INFM-CNR-SOFT, Università di Roma La Sapienza, Piazzale A. Moro 2, 00185 Roma, Italy

(Received 30 June 2006; accepted 18 October 2006; published online 28 November 2006)

We report extensive Monte Carlo and event-driven molecular dynamics simulations of the fluid and liquid phase of a primitive model for silica recently introduced by Ford *et al.* [J. Chem. Phys. **121**, 8415 (2004)]. We evaluate the isodiffusivity lines in the temperature-density plane to provide an indication of the shape of the glass transition line. Except for large densities, arrest is driven by the onset of the tetrahedral bonding pattern and the resulting dynamics is *strong* in Angell's classification scheme [J. Non-Cryst. Solids **131–133**, 13 (1991)]. We compare structural and dynamic properties with corresponding results of two recently studied primitive models of network forming liquids—a primitive model for water and an angular-constraint-free model of four-coordinated particles—to pin down the role of the geometric constraints associated with bonding. Eventually we discuss the similarities between "glass" formation in network forming liquids and "gel" formation in colloidal dispersions of patchy particles. © *2006 American Institute of Physics*. [DOI: 10.1063/1.2393239]

I. INTRODUCTION

Primitive models for atomic and molecular liquids have been and currently are very valuable in the study of the structure and of the thermodynamic properties of several compounds.[1–4] In most cases, primitive models condense the interparticle repulsion in a hard-core potential, while attractive interactions are modeled as simple well potentials. An ingenious choice of the hard-core diameters and of the location and number of the well sites generates models which are able to reproduce many of the essential features of the liquid (and sometimes of the crystal[5,6]) states, despite their intrinsic simplicity. From a theoretical point of view, primitive models are particularly useful, since they allow for a close comparison between theoretical predictions and numerical "exact" results. It is not a coincidence that several novel approaches to the physics of liquids (including critical phenomena and liquid-solid first order phase transitions) are first tested against these models before being extended to more complicated continuous potentials.

Primitive models are relevant not only in the study of liquids, but more generally in the study of colloidal systems, especially when the solvent properties are neglected and colloidal particles are represented as units interacting via an effective potential.[7] Also in colloidal physics, despite the severe approximations, simple hard-sphere and square well models[8–10] have been of significant use in deepening our understanding of the essence of the equilibrium liquid state and of the glass transition. The relevance of these models to colloidal physics is expected to grow in the near future, when the newly synthesized colloidal particles with patterns of sticky patches on their surfaces will be produced in large quantities.[11–13]

A recent line of investigation[14] has called attention on the similarities between glass formation in network forming liquids and gels made by particles with limited valency.[15–18]

While in simple liquids molecules are commonly surrounded by up to 12 neighbors, in network forming liquids, the average coordination is significantly smaller, down to four for the case of silica and water. The interaction strength between the *bonded* nearest neighbors is often significantly larger than the interactions with the remaining molecules. An important thermodynamic consequence of the limited valency is the progressive increase in the region of stability of the liquid phase[15,19] on progressively decreasing the maximum number of interacting neighbors.

Particles interacting only with attractive spherical potentials (beside the hard-core repulsion) cannot form "equilibrium" ideal gels,[20,21] since phase separation prevents the possibility of reaching a homogeneous state at low T, where the lifetime of the bond would be sufficiently long to provide a finite elasticity to the structure. In contrast, limited valency liquids can be cooled down to very small temperatures and meet the kinetic arrest boundaries, without encountering the liquid-gas phase separation boundary in a much larger window of densities. Accordingly, in network forming liquids the slowing down on approaching the glass transition can be

[a)]Electronic mail: cristiano.demichele@phys.uniroma1.it

interpreted as the molecular counterpart of the gelation process in colloidal systems with limited valence. It has also been suggested that the bond energy sets a well defined energy scale in all microscopic processes and induces an Arrhenius dependence of the T dependence of all characteristic times.[16] Limited valence gels, similar to network forming liquids, are expected to be strong in Angell's classification.[22]

To deepen our understanding of this intriguing hypothesis, it is useful to go back to primitive models of network forming liquids and explore their dynamic properties in relation to the fields of thermodynamic stability. Indeed, understanding the loci of dynamic arrest, i.e., the regions in phase space where disordered arrested states can be expected, and the competition between arrest in a nonergodic disordered structure and crystallization in an ordered one, is central in any modeling of material properties. It is fortunate that recently Ford *et al.*[6] have introduced a simple model based on low coordination and strong association for silica, one of the most important network forming materials. This primitive model for silica (PMS) envisions a silicon atom as a hard sphere, whose surface is decorated by four sites, arranged according to a tetrahedral geometry. The oxygen atom is also modeled as a hard sphere, but with only two additional sites. The only (well) attraction takes place between distinct sites of Si and O atoms. Despite the crude modeling, the resulting phase diagram—which includes three solid phases, corresponding to cristobalite, quartz and coesite, a gas and a fluid phase—compares very favorably with the experimental one.[6]

In this article we study static and dynamic properties of this model in the fluid and liquid phases, by performing an extensive set of Monte Carlo (MC) and event-driven molecular dynamics (ED-MD) simulations. Besides structural and thermodynamic properties, we also estimate the line of dynamic arrest in the temperature T–density n plane. With extensive simulations, we equilibrate the system down to temperatures where a full tetrahedral structure develops and most of the particles are fully bonded. When possible, we compare the novel PMS results with corresponding data for two primitive models of four-coordinated particles: a primitive model for water (PMW), introduced by Kolafa and Nezbeda[23] and recently revisited,[14] and a limited valence square well model $N_{\max}$, introduced by Speedy and Debenedetti[24–26] and recently studied as a model for network forming liquids or as a model for gels in a series of papers.[15–17,27,28]

The trend coming out from such a comparison sheds light on the role of the geometric constraints (introduced by bonding) and on how the coupling between bonding and local density may provide a driving force favoring a liquid-liquid phase separation.[29,30]

II. THE MODEL AND NUMERICAL DETAILS

The PMS is a rigid site model in which Si and O atoms (in a 1 to 2 ratio) are modeled as hard spheres complemented by additional sites located at fixed distances from the particle centers (see Fig. 1). The hard-core of the Si–Si repulsive interaction is $\sigma_{\text{Si–Si}} \equiv \sigma$, where σ defines the length scale.

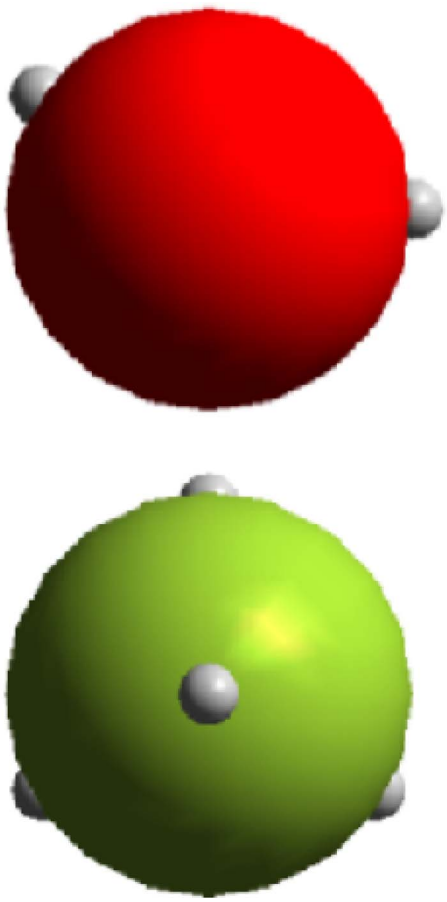

FIG. 1. Three dimensional visualization of the molecular model of silica. Top: O atom modeled as a hard-core particle plus two additional bonding sites, S_1 and S_2, located at distance 0.5σ from the particle center C. The angle $S_1\hat{C}S_2$ is fixed to 145.8°. Bottom: Si atom similarly modeled as a hard-core particle, plus four additional bonding sites located along the direction of a tetrahedral geometry on the surface of the hard sphere, i.e., at distance 0.5σ from the particle center. O and Si sites interact with a well potential of range width $\delta=(1-\sqrt{3}/2)\sigma\approx 0.134\sigma$.

The O–O hard core is defined by $\sigma_{\text{O–O}}=1.6\sigma$, while the Si–O repulsive interaction is again of hard-sphere type but with range $\sigma_{\text{Si–O}}=\sigma$. In this respect, the model defines a nonadditive hard-sphere mixture. The Si particle is decorated with four additional sites located along the direction of a tetrahedral geometry on the surface of the hard sphere, i.e., at distance 0.5σ from the particle center. Each O atom is associated with two additional sites S_1 and S_2 located at distance 0.5σ from the particle center C. The angle $S_1\hat{C}S_2$ is fixed to 145.8°.

The only attractive interaction takes place between pairs of Si and O sites. Sites interact via a well (W) potential u_W, i.e.,

$$u_W = -u_0, \quad r < \delta$$
$$= 0, \quad r > \delta, \tag{1}$$

defined by a small well width $\delta=(1-\sqrt{3}/2)\sigma\approx 0.134\sigma$. The depth of the well potential u_0 defines the energy scale. Pairs of Si–O particles with pair interaction energy equal to $-u_0$ are considered bonded. The value of δ selected in Ref. 6 is slightly larger than the $0.5(\sqrt{5-2\sqrt{3}}-1)\sigma\approx 0.119\sigma$ value

that guarantees the absence of double bonding at the same site due to steric constraints. If the value of δ is chosen in such a way that each site can be engaged at most in one bond, the (negative of the) potential energy of the system E coincides, configuration by configuration, with the number of bonds N_b. Similarly, the fully bonded state coincides with the ground state of the system in which each Si is involved in exactly four bonds. Hence the ground state energy is $E_{gs}=-4$ per Si particle. In the present model, the choice of δ would in principle allow for double bonding at the same site, as alluded to previously. Despite this theoretical possibility, we have checked that this rare event of double bonding never takes place in the present study and hence the system potential energy and (the negative of) the total number of bonds are always coincident.

We have studied a system of $N=216$ particles with periodic boundary conditions for several values of the volume V, spanning a wide range of number densities $n \equiv N/V$ and temperatures T, where T is measured in units of u_0 ($k_B=1$). For $n \leqslant 0.15$, we have studied a system of $N=2160$ particles to better calculate the expected onset of critical fluctuations. We perform both MC and ED-MD. In MC, we define a step as an attempt to move each of the N particles. A move is defined as a translation in each direction of a random quantity distributed uniformly between $\pm 0.05\sigma$ and a rotation around a random axis of random angle distributed uniformly between ± 0.5 radiant. Equilibration was performed with MC and monitored via the evolution of the potential energy (a direct measure of the number of bonds in the system). The mean square displacement (MSD) was calculated to guarantee that each particle has diffused on average more than its diameter. We have also controlled that average quantities do not depend on time. In evaluating the MSD we have taken care of subtracting the center of mass displacement, an important correction for the long MC calculations at low T. Indeed, at low T simulations required more than 5×10^9 MC steps, corresponding to several months of CPU time for each investigated state point. We note that at low T we refer to a metastable equilibrium, i.e., equilibrium within the region of phase space corresponding to a disordered arrangement of the system. The true equilibrium state is, of course, the crystal structure. We have not observed any crystallization event during our simulations in the investigated range of densities.

We have also performed ED-MD simulations of the same system, starting from configurations equilibrated with MC. No variation of any average properties was observed between MC and MD. The algorithm implemented to calculate the trajectory of a system of particles interacting by a hard core complemented by one or more site-site well potentials is described in detail in Ref. 14. The only difference with respect to the algorithm illustrated in Ref. 14 is that here three different linked lists have been used for the three possible interactions: Si–Si, Si–O, and O–O. This is necessary in order to guarantee a good computational efficiency since $\sigma_{O-O}=1.6\sigma > \sigma$. In ED-MD, particle masses have been set to $m_{Si}=14$ and $m_O=8$. The moments of inertia have been assumed to have the values $I_{Si}=14$ and $I_O=8$. Time is measured in units of $(m_O\sigma^2/8u_0)^{1/2}$.

We conclude this section by briefly describing the PMW (Ref. 23) and N_{max} (Ref. 15) models. Both models are one-component models. The PMW has a strong tetrahedral character, imposed by the tetrahedral arrangement of four interacting sites. Two of the sites mimic the H atom and the two other sites the two lone pairs. The N_{max} model is an isotropic square well model with an additional constraint on the maximum number of bonds. A model with four-coordinated particles is generated by imposing that the maximum number of particles probing the well of the potential is limited to 4. A fully bonded particles has four neighbors arranged in a tetrahedral geometry in the PMW and in a random geometry in the N_{max}.

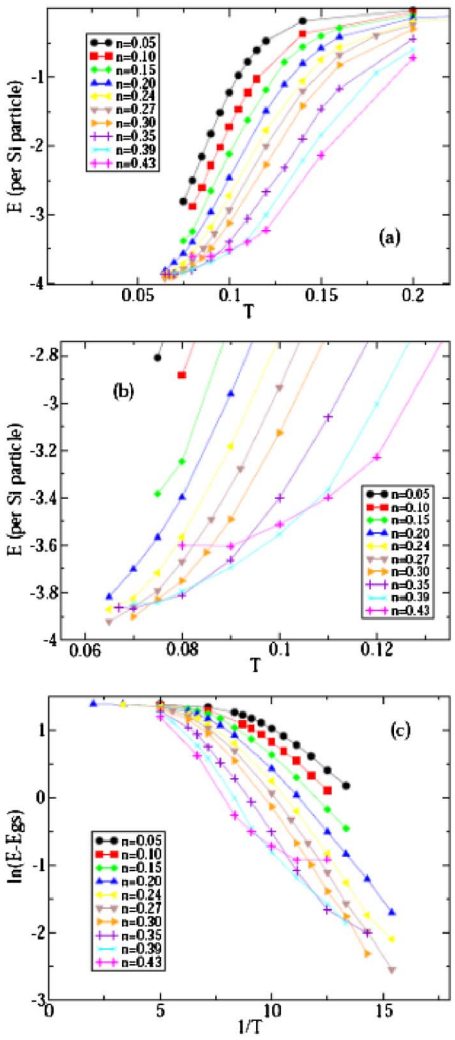

FIG. 2. (a) Potential energy per Si particle E vs temperature T for different isochores. Panel (b) shows an enlargement of the low T part to highlight the approach to the ground state energy $E_{gs}=-4$. Panel (c) shows $E-E_{gs}$ as a function of $1/T$ to show that in the optimal network density region (see text) the behavior of $E-E_{gs}$ follows an Arrhenius law.

III. RESULTS: STATICS

A. Potential energy

The average potential energy of the system per Si particle E is shown in Fig. 2. For $n \lesssim 0.15$, lines stop at $T=0.075$, the lowest T at which the fluid is stable. Indeed, for lower T, liquid-gas separation takes place, as detected by the

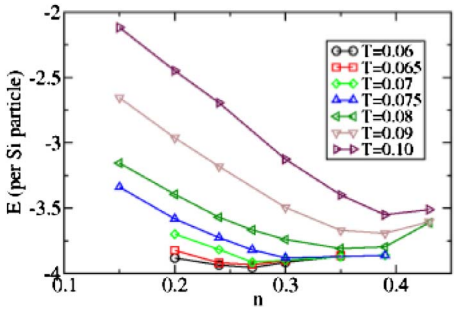

FIG. 3. Potential energy per Si particle vs n along isotherms. Note the minimum that develops around $n \approx 0.27$ at low T.

growth of the structure factor peak at low q. For $n \gtrsim 0.20$, phase separation is never observed in the range of temperatures where it is possible to achieve equilibration with present computational resources. The enlargement of the low T region [Fig. 2(b)] shows that in the region of densities $0.24 \lesssim n \lesssim 0.30$ the potential energy approaches the ground state energy $E_{gs}=-4$, suggesting that a fully connected network of bonds develops on cooling. Outside the range $0.24 \lesssim n \lesssim 0.30$, as $T \to 0$, the energy does not appear to approach E_{gs}. The region $0.24 \lesssim n \lesssim 0.30$ defines the optimal network density region,[14] i.e. the range of n values where a fully bonded state can be reached at low T. For densities lower or higher than the optimal one, the formation of a fully connected network is hampered by geometric constraints: at lower n, the large interparticle distance acts against the possibility of forming a fully connected network, while at large n, packing constraints promoting close packing configurations are inconsistent with the tetrahedral bonding geometry. These features introduce a significant coupling between the maximum number of bonds (and hence energy) and density. It is interesting to observe that, compared to the previously studied PMW case,[14] the region of optimal densities is wider in PMS due to the fact that the bond is mediated by the O particles and that the bonding sites on the O particles are not located along a diameter.

The possibility of reaching the ground state energy in the optimal network density region suggests that, indeed, the equilibrium state at $T=0$ is a disordered fully connected network. In the above sentence, the word "equilibrium" is meant to stress that the system—while being in metastable equilibrium with respect to the crystal state—manages to equilibrate in the restricted part of the configuration space associated with liquid microstates. Support for this hypothesis comes from the T dependence of the energy at low T. As shown in Fig. 3(c), in the region $0.24 \lesssim n \lesssim 0.30$ the energy per Si particle is very well described by the Arrhenius law $E - E_{gs} \sim e^{-E_a/T}$, where $E_a \approx 0.5$ is the activation energy and $E_{gs}=-4$ is the $T=0$ limit. The validity of the Arrhenius law for the energy has been observed also in simulations of more sophisticated models of silica[31] and water.[30] Different from the case of continuous potentials, primitive models do not require any fitting of the ground state energy. It is important to stress that, despite the disorder intrinsic in the liquid state, it appears still possible to fully satisfy the bonds in a disordered homogeneous structure, i.e., it is possible to reach the perfect random tetrahedral continuous network[32] continuously cooling the liquid.

The validity of the Arrhenius law has been verified also in the case of other models.[14,15,17] It is worth recalling that an Arrhenius law for the potential energy with $E_a=0.5$ is also a prediction of Wertheim's thermodynamic perturbation theory,[33,34] a theory developed under the assumption of completely uncorrelated bonding sites. While in the PMS and in the N_{max} model[15] $E_a \approx 0.5$, in the PMW case $E_a \approx 1$. The introduction of the O particle as a bond mediator appears to provide sufficient flexibility in bonding to release the strong geometric constraint imposed by the strict tetrahedral geometry of the PMW.

Figure 3 shows the n dependence of E along isotherms to highlight the presence of the minimum in the density dependence of the energy which develops at low T. The minimum is located in the region $0.24 \lesssim n \lesssim 0.30$ where density allows for the development of a fully bonded tetrahedral network. Figure 3 also shows that a region of weak negative curvature in $E(n)|_T$ develops just outside the optimal density region (i.e., $0.27 \lesssim n \lesssim 0.4$), suggesting that the formation of the network and the coupling between density and energy may act as a driving force for a thermodynamic destabilization of the liquid, favoring the possibility of a liquid-liquid phase transition.[29,30]

It is interesting to compare the density in this optimal region with the density of a diamond crystal. This comparison can be done defining a reduced scaled density n_s as the ratio between the number of four-coordinated particles (the sites of the network) and the volume measured in units of bond distance d_b. In these units, the scaled density for the close packed diamond structure is $n_s^{diamond} \approx 0.65$. From the parameters of the PMS, the expected bond distance between two Si particles bonded via a common O particle is approximatively $d_b = 1.91\sigma$. If one focuses only on the Si atoms (considering the oxygen only as a bond mediator), then the network site number density is reduced by a factor of 3 as compared to the system n. Then the range $0.24 \lesssim n \lesssim 0.30$ converts to a scaled density $n_s = (n/3)(d_b/\sigma)^3 \approx 2.32n$ in the region $0.56 \lesssim n_s \lesssim 0.69$, suggesting that the region of optimal network densities is located around the diamond crystal density.

B. Structure

We start by focusing on the geometry of the Si tetrahedral network. Figure 4 shows the Si–Si–Si angle (θ) distribution at a state point in the optimal density region at low T. It has been recognized in the past that this distribution provides relevant information on the topological properties of tetrahedral networks and helps in quantifying the quality of the tetrahedral structure.[35,36] For the PMS, the distribution extends from 70° to 160°, peaking around 90°. The average value is $\bar{\theta}=107.7$ and the variance is $\sigma_\theta=20.5$. It is instructive to compare the PMS distribution with the distribution found in the PMW and N_{max} models, two related primitive models for four coordinated networks. In the case of PMW, the distribution is highly peaked, with $\bar{\theta}=109$ and $\sigma_\theta=12.0$,

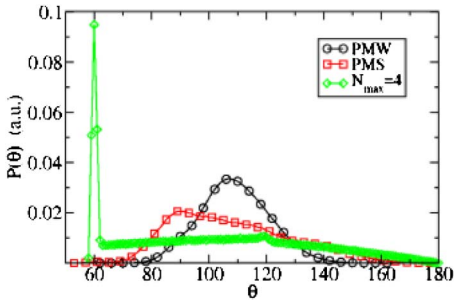

FIG. 4. Distribution of the angle θ between connected triplets of particles for the PMS, PMW, and $N_{\max}=4$ models. In the case of PMS, θ is the Si–Si–Si angle; in the case of PMW and $N_{\max}=4$ models θ is the particle-particle-particle angle.

in agreement with the highly directional character of the interactions. The opposite $N_{\max}$ case is described by a very wide angle distribution, with $\bar{\theta}=100$ and $\sigma_\theta=32$. Different from the PMS and PMW models, in the $N_{\max}$ model configurations with touching triplets of spheres ($\theta\approx 60$) are also found, since angular constraints are missing.

While our aim is not the general comparison between the present model and silica, for which more realistic potentials are available,[37] it is interesting to look at the structure of the system in the optimal network region and compare it with the structure generated by more realistic potentials. Detailed information on the structure of the system on cooling are contained in the particle-particle radial distribution function $g_{\alpha,\beta}(r)$ and in its Fourier transform, the particle-particle structure factor $S_{\alpha,\beta}(q)$ (where α and β label the different particle species). Figure 5 shows the three partial radial distribution functions and compares them with data from Ref. 31. The corresponding comparison in q space is shown in

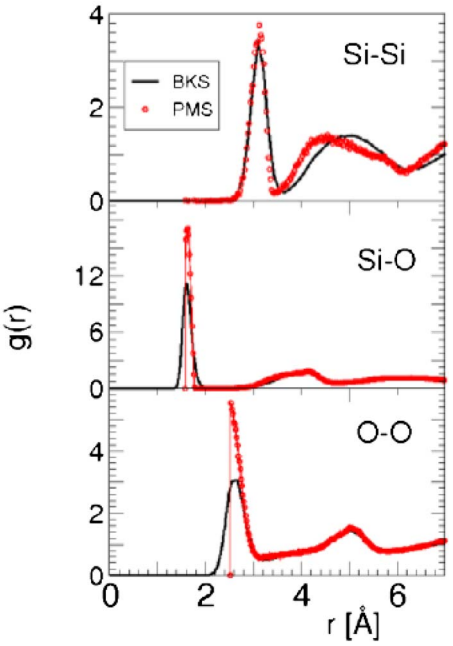

FIG. 5. Radial distribution functions $g(r)$ for Si–Si, O–O, and Si–O at $n=0.30$ and $T=0.07$ (symbols). Lines are results for the BKS silica (Ref. 37) from Ref. 31 at $T=2750$ K. Note that in performing the comparison, σ has been fixed to $\sigma=1.574$ Å.

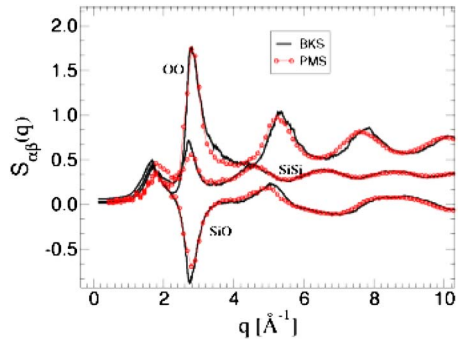

FIG. 6. Partial structure factors $S_{\alpha,\beta}$ (with α and β labeling the particle types [Si,O]) at $n=0.30$ and $T=0.07$. Lines are results for the BKS silica from Ref. 31 at $T=2750$ K. Note that in performing the comparison, σ has been fixed to $\sigma=1.572$ Å.

Fig. 6. It appears that the PMS is able to capture the structure of the tetrahedral network to a good extent. This also suggests that simulations with the PMS can be used as a tool for generating highly bonded configurations which could be used as input for simulation based on realistic potentials.

IV. DYNAMICS

In this section we focus on the dynamic properties of the model, and in particular on the dynamics of Si particles, to put an emphasis on the dynamics of the tetrahedral network. In this respect, the O particles provide the bonds between the nodes of the Si network.

A. Mean square displacement

Figure 7 shows the MSD of the Si particles at one selected n. The behavior of the MSD is characteristic of systems approaching an arrested state. The MSD shows an initial ballistic region, following a low T by a plateau, and, for very long times, a crossover to a diffusive dependence. It is interesting to observe that the height of the plateau, which can be operatively defined as the point in which the MSD versus $\ln(t)$ curve changes concavity, decreases with T. This suggests that, in the studied interval, the localization length associated with the single particle dynamics changes with T. In the present model, the restriction of the cage cannot be

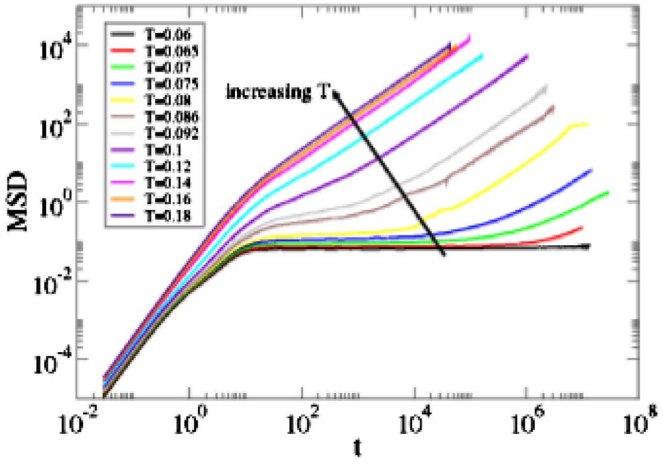

FIG. 7. MSD vs T for Si particles at $n=0.27$.

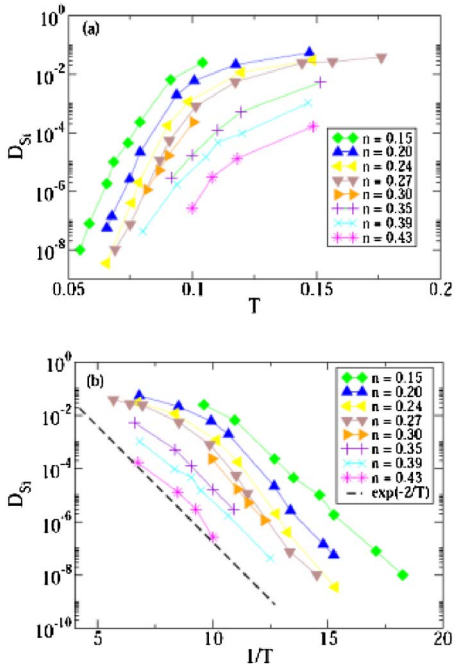

FIG. 8. Temperature dependence of the diffusion coefficient of the Si particles D_{Si} at all studied densities. (a) D_{Si} vs T. (b) D_{Si} vs $1/T$.

associated with a thermally induced decrease of the vibrational amplitudes (as is the case of continuous potentials) and thus signals an effective reduction of the explored volume in the cage due to a progressive development of a bonding pattern. Changes in the particle localization length in PMS are larger than the one observed in the van Beest–Kramer–van Santen (BKS) silica. One possible explanation is that in the present model, floppy modes are strictly at zero frequency (due to the discrete nature of the bonding) and hence give rise to larger amplitude motions as compared to continuous potentials.

B. Diffusion coefficient

The MSD long time limit provides a measure of the diffusion coefficient D. Figure 8 shows that with present numerical resources, the slowing down of the dynamics in this model can be studied over more than six orders of magnitude. While at high T diffusion becomes T independent (an evidence that n is the only relevant variable at high T), on cooling $D(T)$ crosses to a T dependence consistent with an activated law. The linearity of $\log(D)$ vs $1/T$ is very striking in the region of the optimal number densities, where an unconstrained tetrahedral network can form at low T. The activation energy of the diffusion process is close to 2.5. The diffusion of O particles is faster than that of Si particles and follows the same qualitative behavior, crossing to an Arrhenius law at low T, but with an activation energy a factor of 1.7 smaller as compared to Si particles. We note that in BKS silica[31] the ratio of the two activation energies is only 1.1.

In agreement with previously investigated models of network liquids,[30,31,38] slow dynamics in the optimal network region appears to be controlled by activated processes. This suggests that strong-liquid behavior, in Angell's classification scheme, is indeed intimately connected to the limited valency of the interparticle interaction potential. Compared with the PMW data, no diffusion anomalies are observed; i.e., diffusion along isotherms always monotonically decreases on increasing n. In the PMW case, at low T both diffusion minima and diffusion maxima have been observed. This difference can be understood in terms of structural properties and is related to the fact that the distribution of tetrahedral angles in PMS is much wider than the corresponding distribution in PMW.

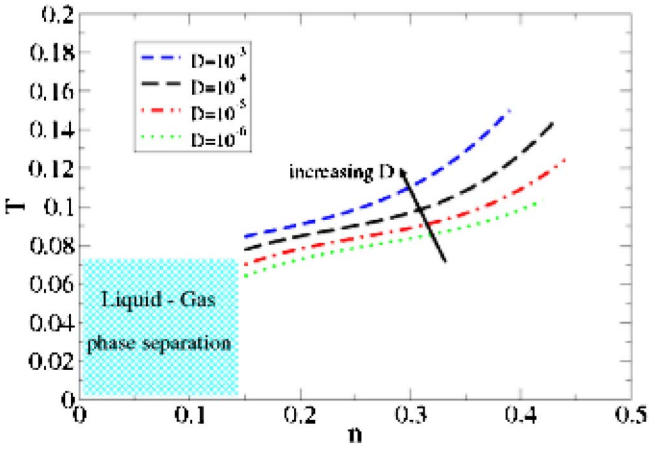

FIG. 9. Isodiffusivity line for Si particles, for four different values of D_{Si}, separated by one decade each. The shaded area schematically indicates the region where liquid-gas phase separation is observed.

C. Isodiffusivity lines

A possible operational way to determine the shape of the dynamic arrest lines is provided by a plot of the isodiffusivity curves in the (T,n) phase diagram.[8,9] For the case of Si particles, these lines are shown in Fig. 9 for three different D values, separated by one order of magnitude each. The isodiffusivity curves start on the left from the gas-liquid spinodal (i.e., cannot be extended to lower densities due to the presence of the unstable region in the phase diagram) and after running essentially parallel to the T axis, start to cross toward a packing controlled dependence. Again, the simplicity of the model does not leave any ambiguity that, at sufficiently large T, the hard-sphere dynamics will be recovered. Hence, isodiffusivity curves will become essentially vertical at larger T.

The shape of the isodiffusivity lines in the present model is similar to that observed in other models of tetrahedrally coordinated particles. The lowest density at which arrest is possible (in a homogeneous, non-phase-separated system) is fixed by the boundary of the spinodal curve. In this respect, this appears to be a common feature of all liquids, independent of the maximum valence. On the other end, it is important to realize that the valence (the number of possible nearest neighbor attractive interactions) controls the location of the high-density side of the spinodal curve. Only when the valence of the particles is reduced below six and the spinodal has moved to small packing fractions can the bond-driven arrest line become accessible and the arrest via activated dynamics be observed.[15]

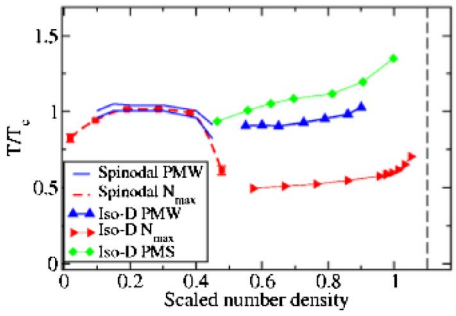

FIG. 10. Comparison between three primitive models for tetrahedral network forming liquids. The dashed line delimitates the HS glass transition at $\phi=0.58$. The three T_c values are 0.22 ($N_{\max}$), 0.1095 (PMW), and 0.075 (PMS). The scaled density n_s (defined as number of four-coordinated particles divided the volume measured in units of the particle-particle distance) coincides with the density in the case of PMW and $N_{\max}$, and it is 2.32 times the PMS number density.

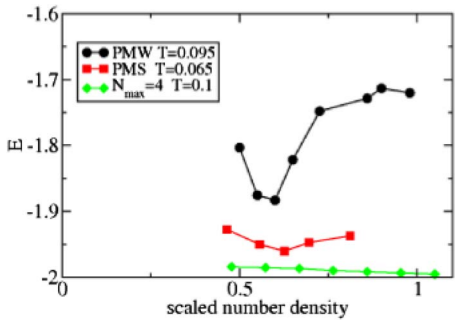

FIG. 11. Density dependence of the potential energy per network particle for the three primitive models. The energy for PMS has been scaled by a factor of 2 since the Si–Si bond requires two bonds via the O particle. The scaled density coincides with the density in the case of PMW and $N_{\max}$, and it is 2.32 times the number density for the PMS.

V. DISCUSSION AND CONCLUSIONS

The aim of the work is to frame the dynamics observed in the primitive model for silica with respect to recent studies of the essential ingredients for slowing down and arrest at low packing fractions and of the connection between glass transition in network forming liquids and gel formation in colloidal particles with patchy interactions. Indeed, patchy colloidal particles of new generation[11–13] may be designed in such a way to closely resemble the primitive model investigated in this work and in previous works. The PMS interpolates between two recently investigated models for tetrahedral network forming liquids, the PMW (Ref. 14) and the $N_{\max}$ (Ref. 15) models, which were selected as the extreme cases of highly spatially correlated directional bonding and completely uncorrelated bonding directions. In the case of PMS, the action of the O particle as mediator of the Si–Si bonding makes it possible to retain the tetrahedral geometry of the Si–Si bonding with an intermediate constraint on the values of the Si–Si–Si angles.

In all three models of four-coordinate particles, liquid-gas phase separation is observed only at low n, below the density at which the open tetrahedral structure of the fully connected network is observed. The three models can be compared in the T-n plane using the scaled density previously defined. A comparison of the phase diagram of the three potentials in this scaled unit is shown in Fig. 10. For all potentials, the liquid-gas phase separation region is confined to the case $n_s \lesssim 0.5$. The figure also shows three isodiffusivity lines, the smallest available isodiffusivity line for each of the three models. The shape of the isodiffusivity lines is also very similar, confirming that in all these models the bond energy scale controls the slowing down between the spinodal and the excluded-volume region.

The coupling between density and extensive bonding has an interesting consequence with respect to the disputed possibility of a liquid-liquid instability, in addition to the gas-liquid phase separation. It has been suggested that a liquid-liquid separation between two disordered liquid states differing in density (and hence in possible bonding patterns) could be a generic feature of all network forming materials with a significant correlation induced by the geometry of the bonds.[39] Also in this respect it is interesting to compare the behavior of the three models, i.e., the behavior of the potential energy per network particle as a function of n_s at low T, shown in Fig. 11. For each potential, the lowest T at which equilibration was achieved is reported. It is striking to see how pronounced the minimum in $E(n)|_T$ is for the PMW case as compared to the weak minimum displayed by the PMS and by the absence of any minimum in $N_{\max}$. The strength of the minimum correlates with the variance of the distribution of the tetrahedral network angles. If the onset of a fully bonded network is possible only for a small range of angles, then the approach of the lowest possible energy state is possible only in a very restricted range of densities. For the case of PMW, where a strong geometric constraint among the bonding sites is present, the region of densities where an almost fully bonded state is reached is localized in a small window around $n_s=0.6$. In the two other cases, where bonds are rather flexible in orientation, fully bonded states are technically possible in a much wider window of densities. Results shown in Fig. 11 thus suggest that the possibility of generating a convex n dependence of the energy (and hence a destabilizing contribution to the free energy of the system and the possibility of a liquid-liquid critical point) is intimately connected to the bonding geometry, since only when the angular bonding energy is sufficiently restricted does full bonding requires a well defined optimal density, generating a strong coupling between energy and density.

An interesting question is posed by the leading arrest mechanism in different parts of the phase diagram. While there is no doubt about the fact that at large n packing constraints (or more generally the shape of the repulsive potential) controls arrest and that at low packing fraction the bonding energy controls arrest, it is still unclear if the two arrest mechanisms cross over continuously from one to the other (in which case we would be entitled to call glasses all arrested states) or if the two arrest mechanisms are intrinsically different and require different names (in which case one would be tempted to define a glass an arrested state at large n and a *gel* an arrested state at small n). From the simulation, it appears rather clearly that (i) the slowing down of the dynamics at small n is characterized by activated dynamics; i.e., it is characteristic of strong glass-forming liquids. Also, (ii) the slowing down of the dynamics along isochores can be

divided into three parts: a constant high T part, a crossover intermediate part and an Arrhenius low T part. The existence of a low T Arrhenius part has the profound consequence that, technically, the arrest line is located at $T=0$. If this is the case, then one would rather imagine that the packing-driven arrest line meets the $T=0$ bond-driven arrest line at a finite n, providing support to the possibility of a discontinuous behavior. On the other end, it is important to recall the evidence presented in the literature of the possibility of interpreting the crossover dynamics observed in more realistic models of tetrahedral forming liquids as the BKS model for silica[31,38] and the extended simple point charge (SPC/E) model for water[40–43] in terms of ideal mode-coupling theory. While a mode coupling theory comparison is impracticable for the present model due to the nonsphericity of the interaction potential, the cited results for BKS and SPC/E support the possibility that at least the crossover from packing to bonding can be captured by a unique theoretical approach.

A final consideration concerns the possibility of calculating in a numerical exact way, along the lines of Refs. 16 and 27, the configurational entropy of this model, especially around the optimal density where the fully bonded state is almost reached within the simulation time. A comparison between the estimate based on the BKS potential[38,44] and the PMS can help resolve the functional form of the density of states and the connections between low-temperature activated dynamics and landscape properties.[45] Work in this direction is underway.

ACKNOWLEDGMENTS

We thank E. Zaccarelli and N. Mousseau for discussions. We acknowledge support from MIUR-COFIN, MIUR-FIRP, and CRTN-CT-2003-504712.

[1] G. Stell, K. C. Wu, and B. Larsen, Phys. Rev. Lett. **37**, 1369 (1976).
[2] I. Nezbeda, Mol. Phys. **99**, 1631 (2001).
[3] I. Nezbeda, Mol. Phys. **103**, 59 (2005).
[4] P. I. C. Teixeira, J. M. Tavares, and M. M. Telo da Gama, J. Phys.: Condens. Matter **12**, 411 (2000).
[5] C. Vega and P. A. Monson, J. Chem. Phys. **109**, 9938 (1998).
[6] M. H. Ford, S. M. Auerbach, and P. A. Monson, J. Chem. Phys. **121**, 8415 (2004).
[7] C. Likos, Phys. Rep. **348**, 267 (2001).
[8] G. Foffi, K. A. Dawson, S. V. Buldrey, F. Sciortino, E. Zaccarelli, and P. Tartaglia, Phys. Rev. E **65**, 050802 (2002).
[9] E. Zaccarelli, G. Foffi, K. A. Dawson, S. V. Buldrey, F. Sciortino, and P. Tartaglia, Phys. Rev. E **66**, 041402 (2002).
[10] F. Sciortino and P. Tartaglia, Adv. Phys. **54**, 471 (2005).
[11] V. N. Manoharan, M. T. Elsesser, and D. J. Pine, Science **301**, 483 (2003).
[12] D. Zerrouki, B. Rotenberg, S. Abramson, J. Baudry, C. Goubault, F. Leal-Calderon, D. J. Pine, and J. Bibette, Langmuir **22**, 57 (2006).
[13] G. Zhang, D. Wang, and H. Möhwald, Nano Lett. **5**, 143 (2005).
[14] C. De Michele, S. Gabrielli, P. Tartaglia, and F. Sciortino, J. Phys. Chem. B **110**, 8064 (2006).
[15] E. Zaccarelli, S. V. Buldyrev, E. La Nave, A. J. Moreno, I. Saika-Voivod, F. Sciortino, and P. Tartaglia, Phys. Rev. Lett. **94**, 218301 (2005).
[16] A. J. Moreno, S. V. Buldyrev, E. La Nave, I. Saika-Voivod, F. Sciortino, P. Tartaglia, and E. Zaccarelli, Phys. Rev. Lett. **95**, 157802 (2005).
[17] E. Zaccarelli, I. S. Voivod, S. V. Buldyrev, A. J. Moreno, P. Tartaglia, and F. Sciortino, J. Chem. Phys. **124**, 124908 (2006).
[18] F. W. Starr and F. Sciortino, J. Phys.: Condens. Matter **18**, L347 (2006).
[19] E. Bianchi, J. Largo, P. Tartaglia, E. Zaccarelli, and F. Sciortino, Phys. Rev. Lett. **97**, 168301 (2006).
[20] G. Foffi, C. De Michele, F. Sciortino, and P. Tartaglia, Phys. Rev. Lett. **94**, 078301 (2005).
[21] F. Sciortino, S. V. Buldyrev, C. De Michele *et al.*, Comput. Phys. Commun. **169**, 166 (2005).
[22] C. A. Angell, J. Non-Cryst. Solids **131–133**, 13 (1991).
[23] J. Kolafa and I. Nezbeda, Mol. Phys. **61**, 161 (1987).
[24] R. J. Speedy and P. G. Debenedetti, Mol. Phys. **81**, 1293 (1994).
[25] R. J. Speedy and P. G. Debenedetti, Mol. Phys. **86**, 1375 (1995).
[26] R. J. Speedy and P. G. Debenedetti, Mol. Phys. **88**, 1293 (1996).
[27] A. J. Moreno, I. Saika-Voivod, E. Zaccarelli, E. La Nave, S. Buldyrev, P. Tartaglia, and F. Sciortino, J. Chem. Phys. **124**, 204509 (2006).
[28] E. Zaccarelli, I. Saika-Voivod, A. Moreno, E. La Nave, S. Buldyrev, F. Sciortino, and P. Tartaglia, J. Phys.: Condens. Matter **18**, S2373 (2006).
[29] P. H. Poole, F. Sciortino, U. Essmann, and H. E. Stanley, Nature (London) **360**, 324 (1992).
[30] P. Poole, I. Saika-Voivod, and F. Sciortino, J. Phys.: Condens. Matter **17**, L431 (2005).
[31] J. Horbach and W. Kob, Phys. Rev. B **60**, 3169 (1999).
[32] W. H. Zacariasen, J. Am. Chem. Soc. **54**, 3841 (1932).
[33] M. S. Wertheim, J. Stat. Phys. **35**, 19 (1984).
[34] M. S. Wertheim, J. Stat. Phys. **35**, 35 (1984).
[35] N. Mousseau and L. J. Lewis, Phys. Rev. Lett. **78**, 1484 (1997).
[36] G. T. Barkema and N. Mousseau, Phys. Rev. B **62**, 4985 (2000).
[37] B. H. van Beest, G. J. Kramer, and R. A. van Santen, Phys. Rev. Lett. **64**, 1955 (1990).
[38] I. Saika-Voivod, P. H. Poole, and F. Sciortino, Nature (London) **412**, 514 (2001).
[39] P. H. Poole, T. Grande, C. A. Angell, and P. F. McMillan, Science **275**, 322 (1997).
[40] F. Sciortino, P. Gallo, P. Tartaglia, and S. H. Chen, Phys. Rev. E **54**, 6331 (1996).
[41] F. Sciortino, L. Fabbian, S. H. Chen, and P. Tartaglia, Phys. Rev. E **56**, 5397 (1997).
[42] F. W. Starr, F. Sciortino, and H. E. Stanley, Phys. Rev. E **60**, 6757 (1999).
[43] L. Fabbian, A. Latz, R. Schilling, F. Sciortino, P. Tartaglia, and C. Theis, Phys. Rev. E **60**, 5768 (1999).
[44] A. Saksaengwijit and A. Heuer, Phys. Rev. Lett. **73**, 061503 (2006).
[45] F. Sciortino, J. Stat. Mech.: Theory Exp. **2005**, 15.